An environmentally friendly method for selective recovery of silver and ITO particles from flexible CIGS solar cells

Sustainable Materials and Technologies 39 (2024) e00844

Contents lists available at ScienceDirect

Sustainable Materials and Technologies

journal homepage: www.elsevier.com/locate/susmat

An environmentally friendly method for selective recovery of silver and ITO particles from flexible CIGS solar cells

Ioanna Teknetzi [a,*], Natalie Click [b], Stellan Holgersson [a], Burçak Ebin [a]

[a] Nuclear Chemistry and Industrial Materials Recycling, Department of Chemistry and Chemical Engineering, Chalmers University of Technology, Gothenburg SE-41258, Sweden
[b] School for Engineering of Matter, Transport and Energy, Arizona State University, Tempe, AZ 85287, USA

ARTICLE INFO

Keywords:
ITO
Silver
CIGS recycling
Ultrasonic leaching
High purity

ABSTRACT

While the share of solar energy harvesting by photovoltaic (PV) systems in electricity production increases, their recycling still remains mainly at an early stage. Therefore, valuable and critical elements like silver (Ag) and indium (In) are lost along with production and end-of-life waste, highlighting the need for simple and sustainable recycling solutions which could be easily implemented by the industry. In this paper, we suggest a simple environmentally friendly method for selective recovery of Ag and Indium Tin Oxide (ITO) particles from flexible Copper Indium Gallium diSelenide (CIGS) solar cells, using two-step ultrasonic (US) leaching with low nitric acid (HNO_3) concentration of 0.1 M. The first step aimed at the selective liberation of ITO through the selective dissolution of the zinc-rich layer underneath, using low US power for 3 min. In the second step, the same conditions as in the first step were applied, but now using high US power for 15 min for removal of the Ag grid lines. Both the ITO and the Ag grid particles were subsequently recovered by filtration and there was no loss of Ag observed in the leachates. By this method, a complete separation of ITO and Ag from the solar cell was achieved, with no changes in their crystal structure and promising purities of about 70.5 wt% and 95.0 wt%, respectively. This new approach opens up a new path for possible direct reuse of these materials in the manufacturing of new PVs, after further purification, with an impressively low need for chemicals.

1. Introduction

Silver is used in a plethora of commercial applications worldwide, with industrial applications having the largest share, about 50%. This share corresponded to 14 ktons in 2021, with 3.2 ktons (22.9% of industrial applications) demanded for PV manufacturing, due to the superior conductivity of metallic Ag [1]. In 2021, the global Ag reserves were estimated to be 530 ktons. At the same time, the total global demand for Ag was 29.7 ktons and the supply 28.3 ktons [1], with 4.9 ktons of them coming from recycling [1,2]. From these numbers it is evident that there is a high demand for Ag, and, since its recycling covers only the 16.5% of it, there are concerns related to the availability of Ag in the future [3].

In the PV sector, Ag is used in the manufacturing of solar cells in the form of a conductive paste for the creation of the conductive contact/grid used to collect the current produced by them [4]. Regarding the recycling of Ag from PV, the current research on its separation from such waste focuses mainly on crystalline silicon (Si) based technologies, due to their large manufacturing share, about 95% in 2022 [5]. Methods for chemical treatment of PV contacts, targeting the dissolution of Ag particles, are common in the literature. Normally, a high concentration of nitric acid (HNO_3) is used, either pure or in mixtures with other acids, and often in combination with high temperatures [6]. However, such conditions, if efficient, are corrosive to equipment and not environmentally friendly. An alternative approach, using US leaching for Ag and other metals present on Si wafers, was studied by Wang et al. [7]. In their work, the goal was not the recovery of Ag, but its removal as impurity from the desired Si wafer, via dissolution in 1–3 M HNO_3. In the case of thin-film PV technology, the literature on their recycling is very limited. To the best of our knowledge, the only article available on Ag recycling from this PV technology is our previous research on CIGS solar cells leaching under relatively mild conditions, with no more than 2 M HNO_3 at room temperature for 24 h [8]. Although that process can be considered to be more environmentally friendly compared to other

* Corresponding author at: Nuclear Chemistry and Industrial Materials Recycling, Energy and Materials Division, Dept. of Chemistry and Chemical Engineering, Chalmers University of Technology, Kemivägen 4, Gothenburg SE - 41258, Sweden.
E-mail address: ioanna.teknetzi@chalmers.se (I. Teknetzi).

https://doi.org/10.1016/j.susmat.2024.e00844
Received 2 December 2023; Received in revised form 12 January 2024; Accepted 29 January 2024
Available online 3 February 2024

methods suggested in the literature for the Si-PVs, its optimization and purification of the dissolved Ag is necessary, because of the high levels of impurities present.

Indium tin oxide (ITO) is a mixed oxide, usually consisting of 90–95 wt% indium oxide (In_2O_3) and 5–10 wt% tin oxide (SnO_2). It is used as a light-transparent conductive coating, mainly in liquid crystal displays (LCDs) [9], but it is also found in PV technologies [8]. Its main compositional element, In, was considered a critical raw material by the EU in 2017. It is also a critical element in "the critical minerals list" of IEA, because of its great economic importance in combination with abundancy issues. The latter is related to the distribution of In reserves mainly in China, difficulties in production (a by-product of zinc) and low concentrations in earth's crust [10,11]. Currently, there is no data available on the world-wide industrial recycling of In [12].

In lab scale, research is mainly conducted today on the recycling of In from ITO found in LCD screens by the use of hydrometallurgical methods. Leaching of the ITO material with inorganic and organic acids has been investigated in these cases [9,11,13]. Some of these studies investigated further the recovery of the leached In by solvent extraction and stripping [9,13], cementation [14] or precipitation [15]. Ultrasonic leaching of ITO from LCD screens has also been tested, aiming to increase the leaching efficiency of In due to the cavitation effect [16,17].

Regarding recycling of ITO or its compositional elements from PV applications, there is a lack of systematic studies, and, when available, the strategy is usually to recover the ITO bound on its original glass substrate, by dissolving the layers above it. In the work by Augustine et al. [18], the recovery of ITO from a perovskite solar cell was studied when using a KOH solution to remove any other material located above the ITO layer. Chen et al. [19] recovered ITO on a glass substrate by first thermally decomposing an encapsulated perovskite solar cell and then opening it up with a knife. The electron-transport layer (ETL) was subsequently washed with 1,2-dichlorobenzene (DCB) and the dissolution of lead halide perovskite film in dimethylformamide (DMF) for subsequent Pb recycling followed. Finally, the hole-transport layer (HTL) and other residuals are mentioned to be washed away, although it is not clear what medium was used. Hu et al. [20] used a polymer solar cell, from which they removed the layers situated above ITO as follows: Ag, MoO_3 and active layer with chloroform, then ZnO with a lactic acid solution of 3% first and then 1%. Other examples of ITO recovery on substrate are those of Elshobaki et al. [21], who used chloroform and water to dissolve the active layer and the poly(3,4) ethylenedioxythiophene):poly(styrenesulfonate) (PEDOT:PSS) layer, respectively, and Dang who used only pure water and ultrasounds to remove the PEDOT:PSS layer [22]. In another research work, the dissolution of a vanadium oxide layer coated immediately above the ITO film on the glass substrate of a fabricated organic PV was achieved by sonication in combination with a dilute base solution [23]. Although all these methods seem to be effective for reuse of ITO-coated substrates, reusing a substrate implies that the recovered materials should be in a perfect condition, free of any defects. Therefore, the reviewed methods have limitations.

To summarize the current situation, both Ag and ITO are valuable materials, commonly used in CIGS solar cells. Today, while the share of the electricity generated by PVs increases rapidly [24], so does manufacturing PV waste, e.g. unqualified manufactured solar cells and solar modules, spent synthesis/manufacturing materials etc. In the future, so will end-of-life waste as well. Ag and ITO could be recovered from this waste. However, very few research articles have investigated the recycling of real CIGS solar cells (ie the substrate with the many different functional layers and the conductive grid) [8] coming from manufacturing waste, instead of other less complex only-CIGS-compound-containing waste materials, like chamber waste and spent sputtering targets. The same is true for waste solar modules (i.e. the solar cell with the encapsulation materials and wiring) [25,26] coming from either manufacturing waste or end-of-life PVs: Currently, research, although still limited, mainly focuses on the recovery of the compositional elements of the CIGS compound, with a special interest in the recovery of the critical In and Ga. The two recovery routes that are usually investigated for the recycling of compositional elements from the CIGS compound in general are i) a first step consisting of thermal treatment, aiming at the recovery of Se, and a later step of acid leaching, aiming atthe dissolution of the rest of the elements [25,27] or ii) a direct leaching step aiming at the dissolution of all the elements [28,29]. Purification and recovery of the various elements should follow in all cases and different methods can be used. A more detailed review of the research which has been conducted on CIGS recycling so far can be found elsewhere [30]. Remarkably, although Ag and ITO are valuable materials, their recovery from CIGS PVs has been neglected so far and even the proposed methods for the recovery of these materials from other PV technologies still present limitations and various drawbacks, as discussed in the previous paragraphs.

The present work, therefore, aims to find a simple, quick and environmentally friendly approach for recovering high purity Ag and In from flexible CIGS solar cells with a stainless steel substrate coming from manufacturing waste. We here investigate a possible advantage of the ability of low concentrations of HNO_3 (0.1 M) to selectively dissolve layers situated underneath the Ag grid and ITO layer, in combination with ultrasounds to liberate the Ag and ITO from the cell and recover them as particles. Low and high power settings of an ultrasonic bath are tested in order to make the recovery as selective and efficient as possible. In this way, both materials can be recovered in the form of the original particles with high purity. Their high purity renders further optimization or purification for achieving the levels required for reuse of the materials in the manufacturing of solar cells easy. Moreover, by separating the Ag and ITO in the beginning of the recycling process, the remaining layers (eg CIGS and back contact) can be recovered in later steps, with better chances of achieving high purity for them as well.

2. Materials and methods

The materials and equipment used in this work are described in this section, as well as the experimental procedures followed. All experiments were performed in triplicates, with each replicate of the same experimental conditions coming from a different solar cell. It should be also clarified that the geometrical surface to liquid ratio (A/L) was used, instead of the solid to liquid ratio, in all experiments, since the mass of the film was very small and, therefore, measurable differences in the mass would only come from the stainless steel substrate and not the film.

2.1. Materials

Concentrated HNO_3 (69%, Suprapur, Merck) and ultra-pure water (Milli-Q, Merck) with a resistivity of 18.2 MΩ•cm were used for all the experiments and analysis of liquid samples. Ethanol (95%, Solveco) was used for the recovery of solid particles from filter papers (by washing the particles off the filter papers) and for washing off any liquid leftovers from particles separated from acid solutions (leachates/digestates).

The flexible CIGS solar cells (15.6×15.6 cm^2) with an Ag conductive grid and a stainless steel substrate were provided by the Swedish solar cell and module manufacturing company Midsummer AB. A short description on the stacking order of the known layers present in the CIGS solar cells used in these experiments is considered necessary, since the relative position of the layers played a key role in the success of the described method. More specifically, based on our previous work with the same samples and the available literature-based knowledge of CIGS solar cell manufacturing [8], the cells used in the experiments were made with a flexible stainless steel substrate on which Mo and W were deposited. Above them, the CIGS absorber layer was found. The buffer and window layers followed. Our previous work proved the presence of a Zn-rich layer here. Finally, the top layer was found to be ITO and then the Ag grid lines were printed on top of it. An illustration of the layers' order is presented in Fig. S1 of the Supplementary Material.

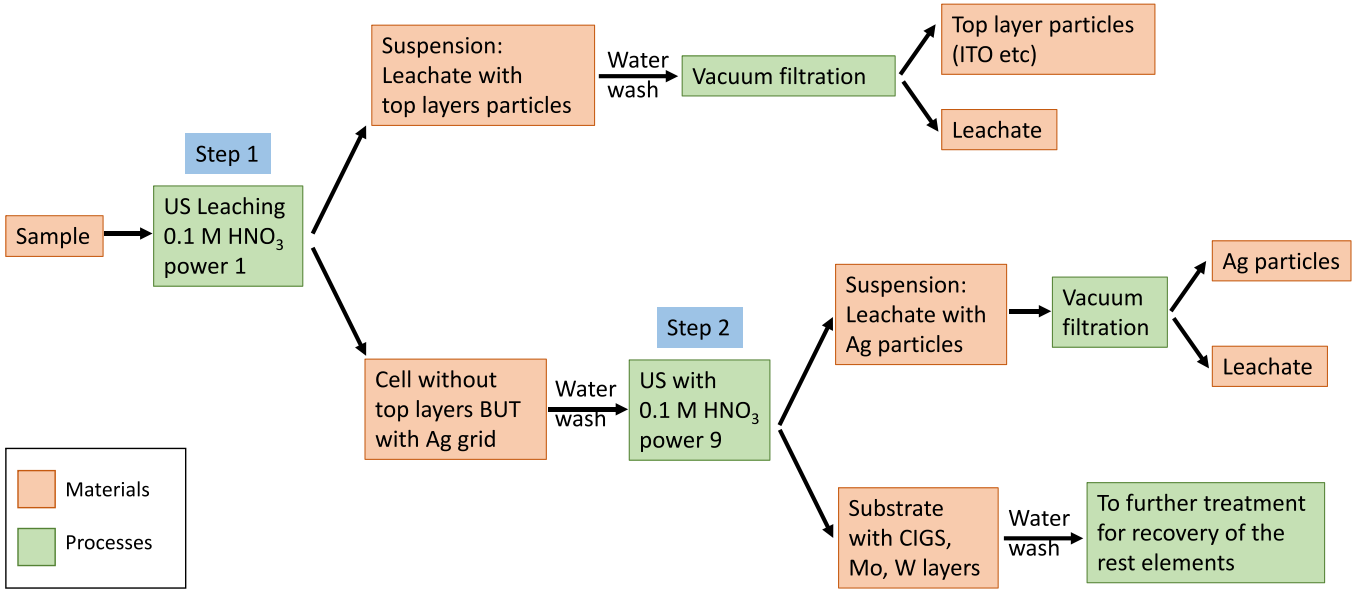

Fig. 1. Flow chart of the final two-step US-leaching process for selective removal of top (ITO-rich) layers in a first step and Ag grid recovery in a second, from flexible CIGS solar cells with an Ag grid and stainless steel substrate.

In our previous work [8], the Zn-rich layer had dissolved completely and selectively in no longer than 1 h in a low concentration of HNO_3, equal to 0.1 M, during conventional leaching with mechanical stirring. The high electropositivity of Zn, as well as the kinetics of its reaction, are believed to be the reasons for that behavior. The observation suggested that a small amount of energy, e.g. from ultrasounds, could be enough to remove any material placed above the dissolved Zn-rich layer, like the ITO, the Ag grid and others.

2.2. Experimental method

In all experiments, US leaching was performed with 90.5 ml of a HNO_3 solution of 0.1 M. The minimum and/or maximum power of an US bath of US frequency equal to 132 kHz and output US power 80 W (USC-THD/HF model by VWR, 230 V version) was used for each experiment. The minimum and maximum power were indicated by the manufacturer as "power 1 for 40% and power 9 for 100% of the maximum power" of the bath.

The solar cell sample used for each replicate was a piece of the whole solar cell, of geometrical surface area equal to 1/8 of that of the whole cell (cut as illustrated in [8]). Each of the samples was immersed in a glass beaker and the beaker was placed in the basket of the US bath, under the experimental summarized in Table S1 of the Supplementary Material.

More specifically, two experiments were performed initially, one at the minimum and one at the maximum US power. When the minimum US power was used, the selective removal of the top layers (ITO-rich) from the cell's surface was checked visually at 1, 2, 4, 6, 8 and 10 min of US leaching, in order for the optimal residence time to be determined. The optimal time in this case was defined as the time required for the achievement of maximum liberation of the top layers with minimum liberation of the Ag grid. On the other hand, when the maximum US power was used, the removal of the Ag grid from the cell was checked visually at 5, 10 and 15 min of US leaching, in order for the optimal residence time to be determined. In this case, the optimal time was defined as the minimum time required for the complete removal of the Ag grid. The reason behind the selection of these power levels for the achievement of the objectives associated with them is discussed in Section S3 of the Supplementary Material. The surface of the treated samples was finally studied under the microscopes.

The optimized time results for selective top layers separation and complete Ag grid removal were then used in the development of an optimal process for recovery of these materials. The flow chart of the process is illustrated in Fig. 1 and the experimental conditions of each step are presented in detail in Table S1 of the Supplementary Material. More specifically, in the 1st process step the sample was US-leached using 0.1 M HNO_3 at power 1, to selectively remove the top layers from the cell, and then the suspension was vacuum filtrated and the recovered particles were washed with MQ water. The leachate and the collected particles were analyzed. The cell piece with the removed top layers was washed well through its immersion in a beaker with MQ water. Then it continued to the 2nd US leaching step of power 9 and a new solution of 0.1 M HNO_3, in order for the Ag grid to be liberated. Again, the suspension was vacuum filtrated and the leachate and the collected particles were analyzed as well. The remaining cell was washed again with MQ water and left to air-dry for future treatment.

2.2.1. Digestion of solid particles for % recovery and wt% purity determination

Three digestion sets were performed, each of them aiming to the determination of one of the following sizes: a) wt% ITO purity, b) wt% Ag purity and c) % Ag recovery. In all cases, a solution of 4 M HNO_3 was used for the digestions at room temperature. Sampling was performed at different time points in order for the progress of the digestion to be checked. The maximum values of the leached amount for each element were used for the calculations. More details on the digestion methodology and conditions are presented in Section S4 of the Supplementary Material.

2.2.2. Instrumentation for analysis

The elemental analysis of the leachates and digestates was performed with Inductively Coupled Plasma – Optical Emission Spectroscopy (ICP-OES, ThermoScientific iCAP PRO Duo), using elemental standards for the elements Ag, Cr, Cu, Fe, Ga, In, Mg, Mo, Se, Sn, Ti, W, Zn (1000 ppm, Inorganic Ventures). An internal standard of 1 ppm Y was added to all samples and standards to ensure the accuracy of the measurements. The morphology of the surface of the treated samples was partly studied with Optical Microscopy (Zeiss Vert.A1). The rest of the morphological as well as qualitative (not quantitative, due to the inherent heterogeneity of samples) elemental analysis of the solid samples (i.e. treated cells and

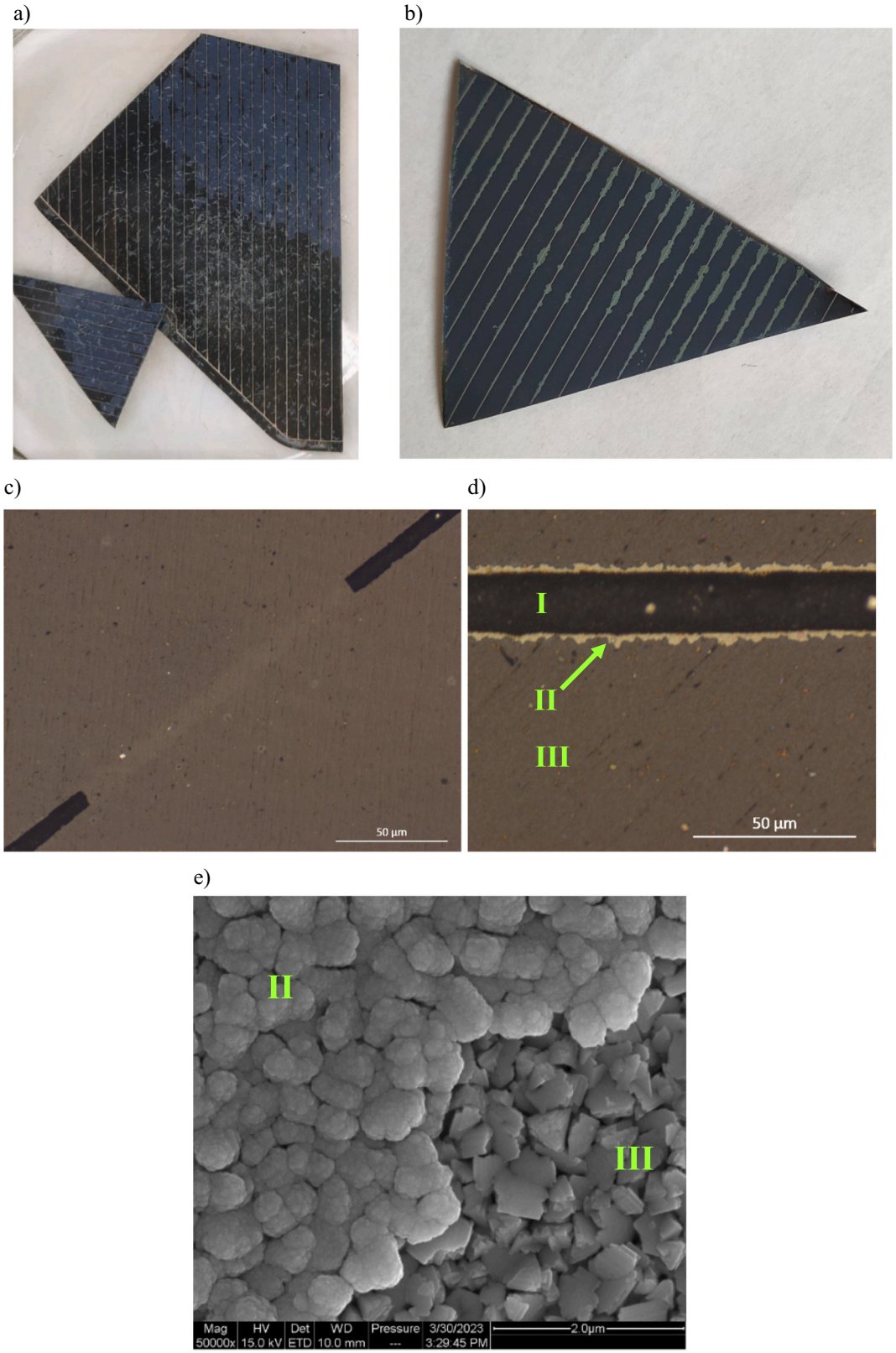

Fig. 2. Results from US-leaching using the minimum US power (Experiment 1USL0.1): a) Cell sample after 1 s with selective partial liberation of the top layers, b) sample treated for 2 min in US, with a small amount of top layers leftover, c) optical microscope image showing the liberation of small pieces from the Ag grid after 6 min, d) magnification of an Ag grid line from (c) with traces of top layers leftovers observed around it and e) SEM image from the border between materials II and III from (d). The areas named I, II and III correspond to Ag grid, top layers leftovers and CIGS layer, respectively.

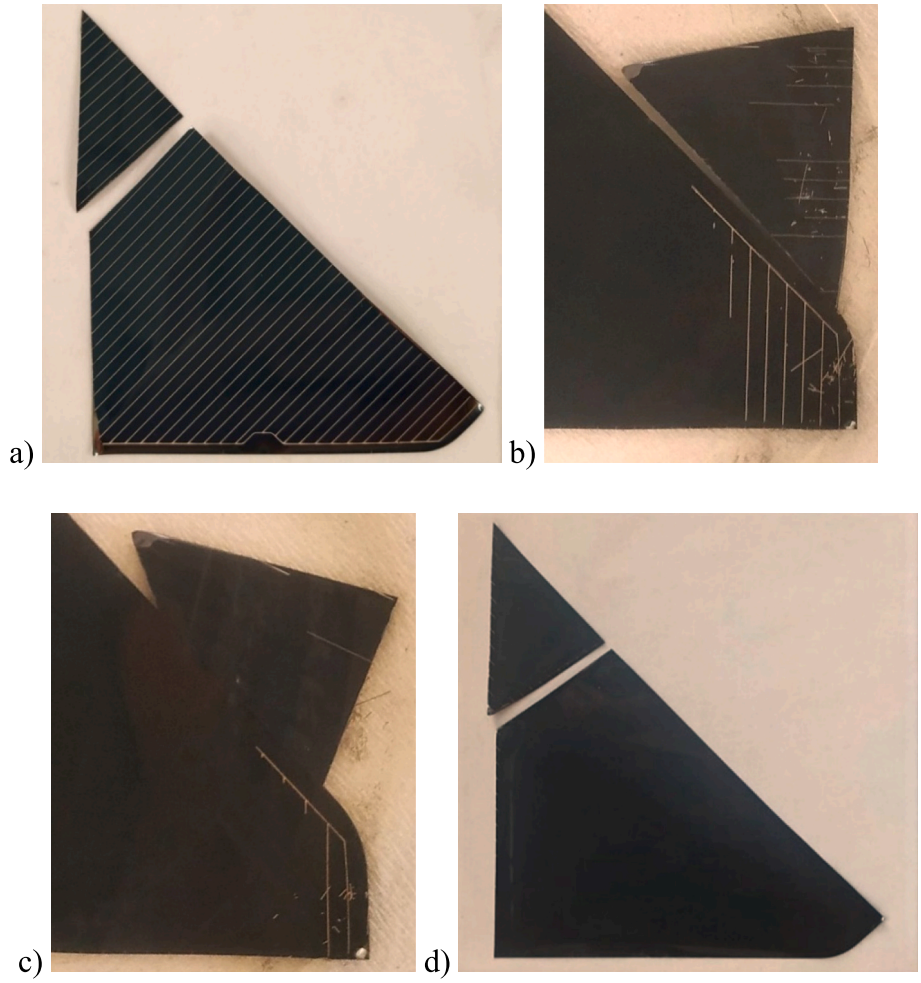

Fig. 3. Cell sample used in the experiments: a) untreated, b) after 5 min, c) 10 min and d) 15 min of US-leaching at maximum US power (Experiment 9USL0.1).

recovered particles) was performed using Scanning Electron Microscopy coupled with Energy Dispersive X-ray Spectroscopy (SEM-EDS, FEI Quanta 200 FEG SEM with an Oxford Instruments X-Max EDS detector). The crystalline phases of the recovered solid particles were identified with an X-Ray Diffractometer (XRD, D8 Discover, Bruker), using Cu K_α radiation. EVA software and JCPDS database were used for that purpose. For the quantification of the organics content in the recovered Ag particles Thermogravimetric Analysis (TGA, TA Intsruments Q500) using air atmosphere was performed.

2.2.3. wt% purity and % recovery calculations

In this paper, the leached mass of element per cell, the wt% ITO purity, wt% Ag purity, as well as the % Ag recovery were calculated as follows:

$$\frac{mass}{cell} = C_{ICP} \bullet DF \bullet V_{solution} \bullet 8 \tag{1}$$

For the calculation of ITO wt% purity, ITO is considered as a mix of In_2O_3 and SnO_2:

$$wt\%ITO purity = 100 \frac{0.5\left(\frac{C_{ICP} \bullet DF \bullet V_{solution}}{Aw}\right)_{In} Mw_{In2O3} + \left(\frac{C_{ICP} \bullet DF \bullet V_{solution}}{Aw}\right)_{Sn} Mw_{SnO2}}{m_{particles}} \tag{2}$$

$$wt\%Ag\ purity = 100 \frac{C_{ICP} \bullet DF \bullet V_{solution}}{m_{particles}} \tag{3}$$

$$\%Ag\ recovery = 100 \frac{(mass/cell)_{meas}}{(mass/cell)_{tot,ref}} \tag{4}$$

The impurity content of element i in the recovered particles was calculated as:

$$wt\%impurity\ i = 100 \frac{C_{ICP} \bullet DF \bullet V_{solution}}{m_{particles}} \tag{5}$$

In all the equations, C_{ICP} is the concentration of the respective element measured with the ICP-OES, DF is the dilution factor used for the same measurement and $V_{solution}$ is the volume of the leaching solution. A multiplication factor of 8 is necessary in (Eq. 1), since the cell was divided into 8 pieces and one of them was used per replicate. The subscript "meas" in (Eq. 4) denotes the mass of Ag per cell recovered from the liberated Ag particles. "tot, ref" in the same equation denotes the total mass of Ag per cell. For the latter, the reference was our previous work [8], in which a total Ag amount of 64.1 ± 4.7 mg/cell was measured after digestion of the cells. The subscript "particles" in (Eq. 3) and (Eq. 5) denotes the total mass of the sample of particles digested in the particular experiment. Finally, Aw and Mw denote the atomic and molar mass [g/mol], respectively.

3. Results and discussion

The results from the experiments aiming at the determination of the optimal residence times under different US powers, as well as the results of the characterization of the liquid and solid fractions from the optimal

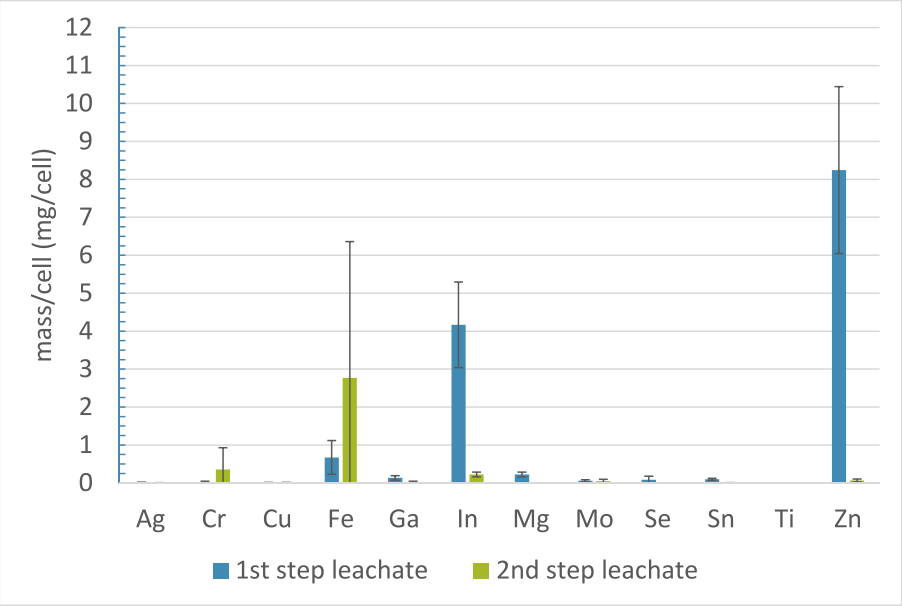

Fig. 4. Elemental analysis of the 1st and 2nd step leachate.

process, are presented here in the order they were performed. The uncertainties in the results are expressed as the standard deviation σ.

3.1. Residence time experiments

When the minimum US power was used (Experiment 1USL0.1), a faster liberation of the top layers was observed compared to the Ag grid lines. As presented in Fig. 2a, taken 1 s after the initiation of the US leaching, first, the top layers broke into smaller pieces and started getting liberated from the surface of the cell. In the same figure, the areas of the cell shown as light blue are the areas with the top layers still attached and the areas that appear black are the ones from which the top layers were liberated, observable as light-colored particles scattered in the solution. No distraction of the Ag grid (white lines) is observable in Fig. 2a. As the residence time increased, some small pieces of the Ag grid were also liberated. The results concluded that 3 min was the optimum time for the maximum removal of top layers without any liberation of the Ag grid. For shorter times, although no liberation of the Ag grid was observed, a small amount of top layers material was still attached to the cell's surface (Fig. 2b). For longer than 3 min treatment times, detachment of some small pieces of the Ag grid was observed (Fig. 2c). At the same time, some traces of the top layers material were still attached around the Ag grid lines, as shown in Fig. 2d-e (the EDS spectra of d is given in Fig. S3 of Supplementary Material). However, there was no observable difference in the removal of these leftovers with residence time after the 4 min. Therefore, the residence time of 3 min was chosen as the optimum for achieving an almost complete and at the same time selective recovery of the ITO-rich top layers.

When the maximum US power was used (Experiment 9USL0.1), complete removal of the Ag grid was possible in 15 min, as can be seen in Fig. 3: before the treatment, the Ag grid could be observed as the white lines on the cell's surface in Fig. 3a. After 5 min of US-leaching, a considerable amount of them had been liberated (Fig. 3b), while after 10 min only a few pieces of them remained attached to the cell (Fig. 3c). Finally, after 15 min, they were not visible anymore, meaning that the Ag grid had been successfully liberated from the cell's surface (Fig. 3d).

It is worth mentioning here that sonication of the sample under exactly the same conditions but with water instead of 0.1 M HNO_3 had no impact on either the top layers or the Ag grid, in terms of liberation of the materials from the cell (Fig. S4 of Supplementary Material). Therefore, the selective dissolution of the Zn-rich layer by an acid solution of low concentration was necessary for the success of the method.

3.2. Optimal process with two US-leaching steps

The optimal time results determined in Section 3.1 were used for the development of the optimal process, consisting of two US-leaching steps of different US power: the 1st step (US-leaching at minimum power) for selective and complete removal of ITO and the 2nd step (US-leaching at maximum power) for complete removal of the Ag grid. The characterization of the ITO- and Ag-rich particles recovered after the respective process steps and their determined wt% purity and % recovery are presented in this section. The composition of the leachates after each step was also analyzed for possible losses of the elements of interest in the acid solution. It is important to clarify here that all the elements mentioned in Section 2.2.2 were measured at all times. If they are not displayed in the given results, it means that their concentrations were below their detection limit.

3.2.1. 1st step of the process: Recovery of ITO

The elemental analysis of the leachate from the 1st step is presented in Fig. 4. The results showed that the elements which were mainly leached were Zn and In, while the concentrations of other metals present were very low. In the case of upscaling of the process, separation and recovery of Zn and In from this stream (eg by selective precipitation or solvent extraction [31] after proper increase of the elemental concentrations) might be beneficial. It is worth noticing that practically no Ag was leached during this step, since its detected concentration in the analyzed samples was close to its detection limit of about 1 ppb.

The recovered top layers particles are presented in Fig. 5a, while their SEM morphology can be observed in Fig. 5b. Their XRD analysis (Fig. 5c) confirmed that the dominant crystalline phase was ITO, while a very minor quantity of pure Sn_2O_3 phase was also detected. Whether the Sn_2O_3 phase was present in the untreated cell too or it was the result of the US-leaching treatment, it was difficult to say. If the latter was the case, the following scenario was possible: Some Sn from the ITO dissolved during the US-leaching, as indicated by the small amount of Sn detected in the leachate of the 1st step of the process in Fig. 4. Then, some of this dissolved Sn precipitated from the leachate as Sn_2O_3, during the process and/or during filtration and rinsing of the (covered with some remaining leachate) particles with water, due to its limited dissolution in HNO_3 [9,11,32].

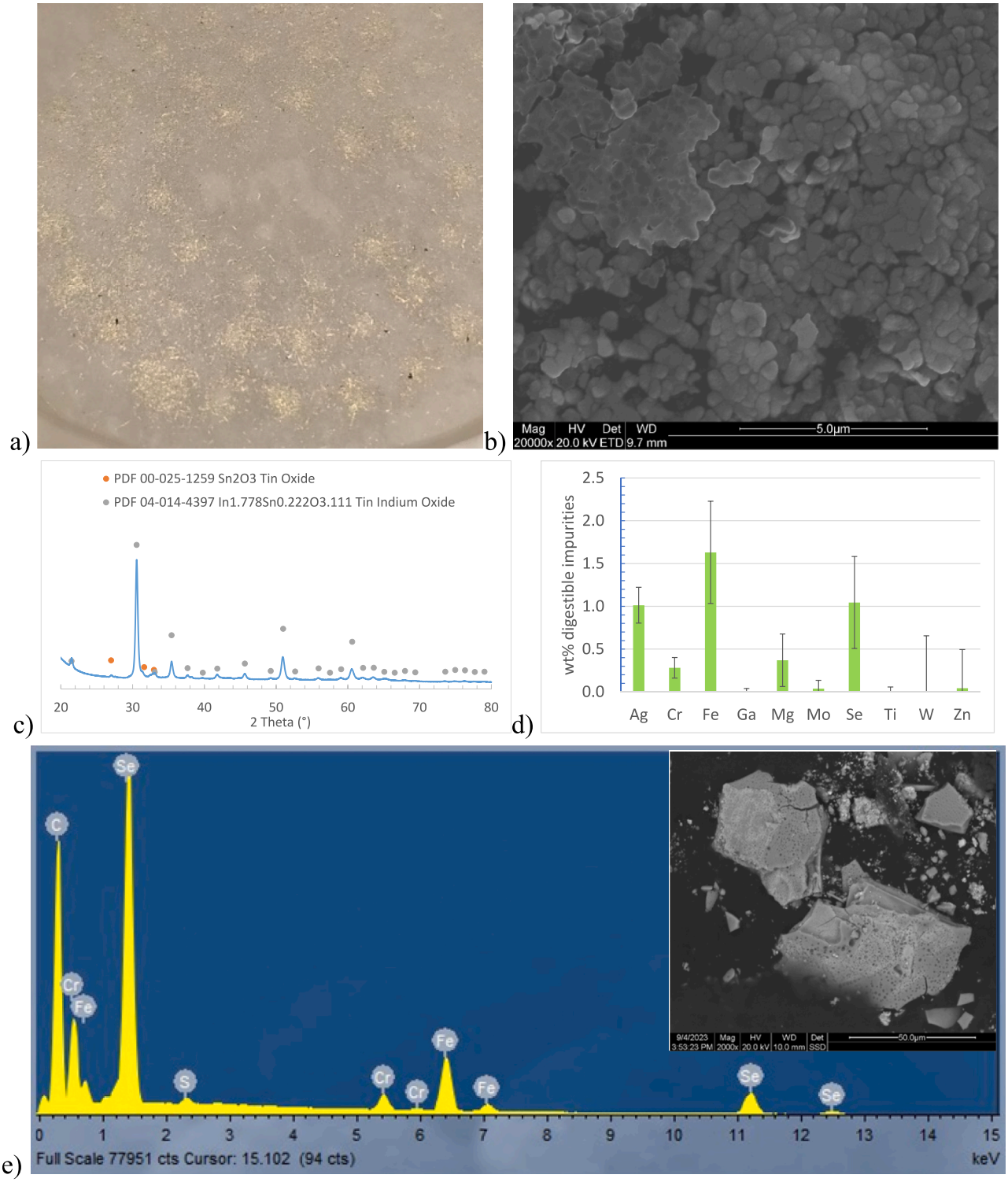

Fig. 5. Analysis of the filtered solid particles from the 1st US-leaching step: a) recovered particles after filtration, b) SEM image showing the morphology of the recovered particles, c) XRD pattern of the crystalline phases, d) elemental analysis of the digestible impurity levels expressed as wt% and e) EDS spectrum of the non-digestible particles shown in the inset. The areas I, II and III correspond to Ag grid, top layers leftovers and CIGS layer, respectively.

The elemental analysis of the recovered ITO-rich particles was determined from their digestion. For calculation purposes of wt% ITO purity, all the In and Sn leached from the digested particles (Figure S5 of the Supplementary Material) were considered as components of ITO, concluding a purity of about 70.36 ± 6.08 wt%. Some small amounts of other digestible elements were also detected with the same method (Fig. 5d). It should be clarified here that since the ICP analysis was performed on liquid samples, it could only quantify the content of an element in a solid sample based on the digestible amount of this particular element. As a consequence, the non-digestible amount could not be quantified. In our case, after the completion of the digestion (assessed in the way discussed in Section S7 of the Supplementary Material), it was observed that a fraction of the particles was left undigested. Based on how low the detected digestible impurity levels were,

Table 1
Average wt% elemental composition of recovered particles.

	Ag	Cr	Cu	Fe	Ga	In	Mg	Mo	Se	Sn	Ti	W	Zn	Organ.	Rest (mainly O, S)
ITO-rich	0.90	0.19	–	1.17	0.04	52.64	0.51	0.07	0.59	5.29	0.03	0.38	0.32	–	<<37.87
Ag-rich	94.96	0.01	0.02	0.03		0.12	0.06		0.07	0.02	–	–	0.02	3.12	1.58

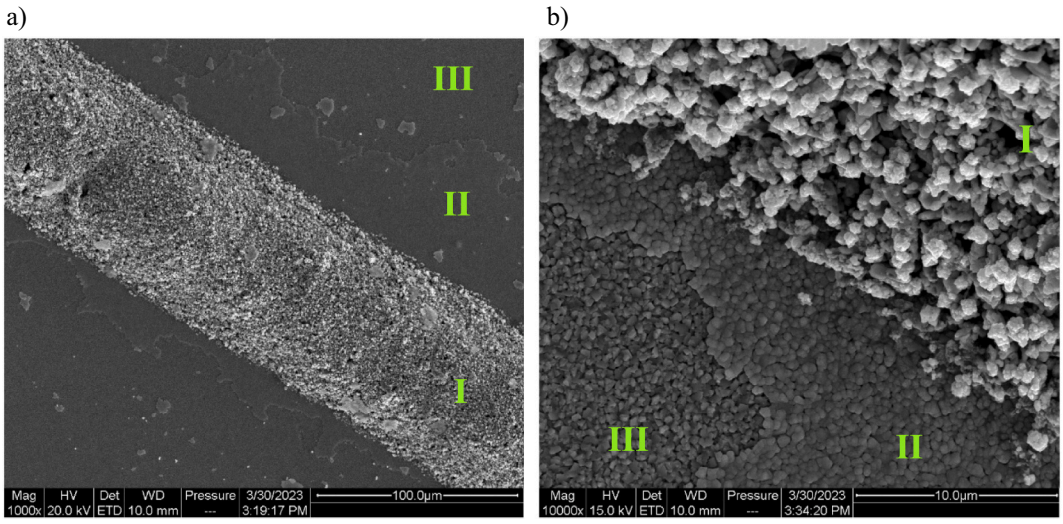

Fig. 6. SEM images at a) lower and b) higher magnification of the area around an Ag grid line after the 1st step of the optimal process, showing traces of top layers materials around the lines. The areas I, II and III correspond to Ag grid, top layers leftovers and CIGS layer, respectively.

the majority of the impurities seemed to originate from the non-digestible material.

SEM-EDS analysis revealed that the non-digestible particles were Se-Fe-Cr rich, with smaller quantities of S (Fig. 5e). Despite their considerable concentration in the sample, their peaks are absent from the XRD pattern of Fig. 5c, probably due to absence of crystallinity and/or lower individual amounts. More SEM images of them are given in Fig. S6 of the Supplementary Material. Since Fe and Cr are not elements used in the film layers, this contamination is expected to come from the stainless steel. It is likely that Se and S containing particles were manufacturing residues stuck on the stainless steel substrate, since both elements are used often in their gas form during manufacturing, to form selenides and sulfides layers [33]. Finally, it is worth mentioning that the Ag amount detected in the recovered ITO-rich particles corresponds to no more than 0.15 wt% of the total Ag in the cell, meaning that any Ag losses were negligible. The average estimated elemental composition of the ITO-rich particles, taking into account both the digested and undigested fractions, is presented in Table 1.

Regarding the % recovery of ITO, it could not be determined quantitatively through a digestion, since the total amount of ITO in the cell was unknown. Its quantification through a total digestion of the whole cell would not be possible, either due to the fact that In (the main component of ITO) is present in other layers as well orbecause the already very small amount of Sn present in the cell (and the challenges in its dissolution) would probably render the determination of total ITO in the cell based on Sn unreliable. For these reasons, its recovery was decided to be determined in a semi-quantitative way, through visual observation combined with study with SEM. Based on these observations, the recovery of ITO was $\geq$99 wt%, since only some traces of it were left around and below the Ag grid lines, as shown in Fig. 6.

Finally, it is worth highliting that any amount of Ag lost in the 1st step (in both the leachate and ITO-rich particles) was of the order of few µg/cell, and thus negligible compared to the total Ag of a few mg/cell.

3.2.2. 2nd step of the process: Recovery of Ag

The elemental analysis of the leachate from the 2nd US-leaching step is presented in Fig. 4. In this step, it was mainly the stainless steel from the substrate that was leached. Some other low concentration impurities were present as well. However, it is important that there was practically no loss of Ag in the leachate of this step either, since its concentration in the analyzed solution was below its detection limit of about 1 ppb.

The Ag particles recovered via filtration after the 2nd US-leaching step are presented in Fig. 7a and their morphology in Fig. 7b. It is noticeable that their size was considerably coarse (tens of µm) and all had the same elongated shape. A higher magnification image of one of those particles, presented in Fig. 7c, revealed that each of them was an aggregate of fine Ag particles of the size of µm or less.

Regarding the purity of the particles, their crystalline phase was identified by XRD as pure Ag in its metal form (Fig. 7d). A considerably high wt% purity of the Ag particles, equal to 94.96 $\pm$ 1.29 wt%, was determined with the ICP-OES after their digestion (the assessment of the completion of the digestion is given in Section S8 of the Supplementary Material). The elemental concentration of other impurities detected with the same method is presented in Fig. 7e. It is worth noticing that the leachable impurities level was very low. The dominant impurity among them, although still only about 0.1 wt%, was In, expected to come from the ITO layers which remained attached to the bottom of the grid lines, as it can be observed in Fig. 7c (area I for Ag and II for In-containing material). The only residues that remained after the digestion were the organics from the Ag paste (Fig. S8 of Supplementary Material) and their content was determined with TGA to be equal to 3.1 wt%, as shown in Fig. 7f. More specifically, during the TGA measurement, Ag oxidized from room temperature until about 200 °C and then started reducing [34]. The burning of organics also took place at temperatures in the reduction region of Ag [35,36]. Organic removal was completed at about 380 °C, resulting to a relative weight difference of 3.1 wt%. The presence of organics and the size and shape of the aggregates suggest that the recovered Ag was actually contained in fragments of the Ag grid, not in the form of individual particles liberated from the grid's organics.

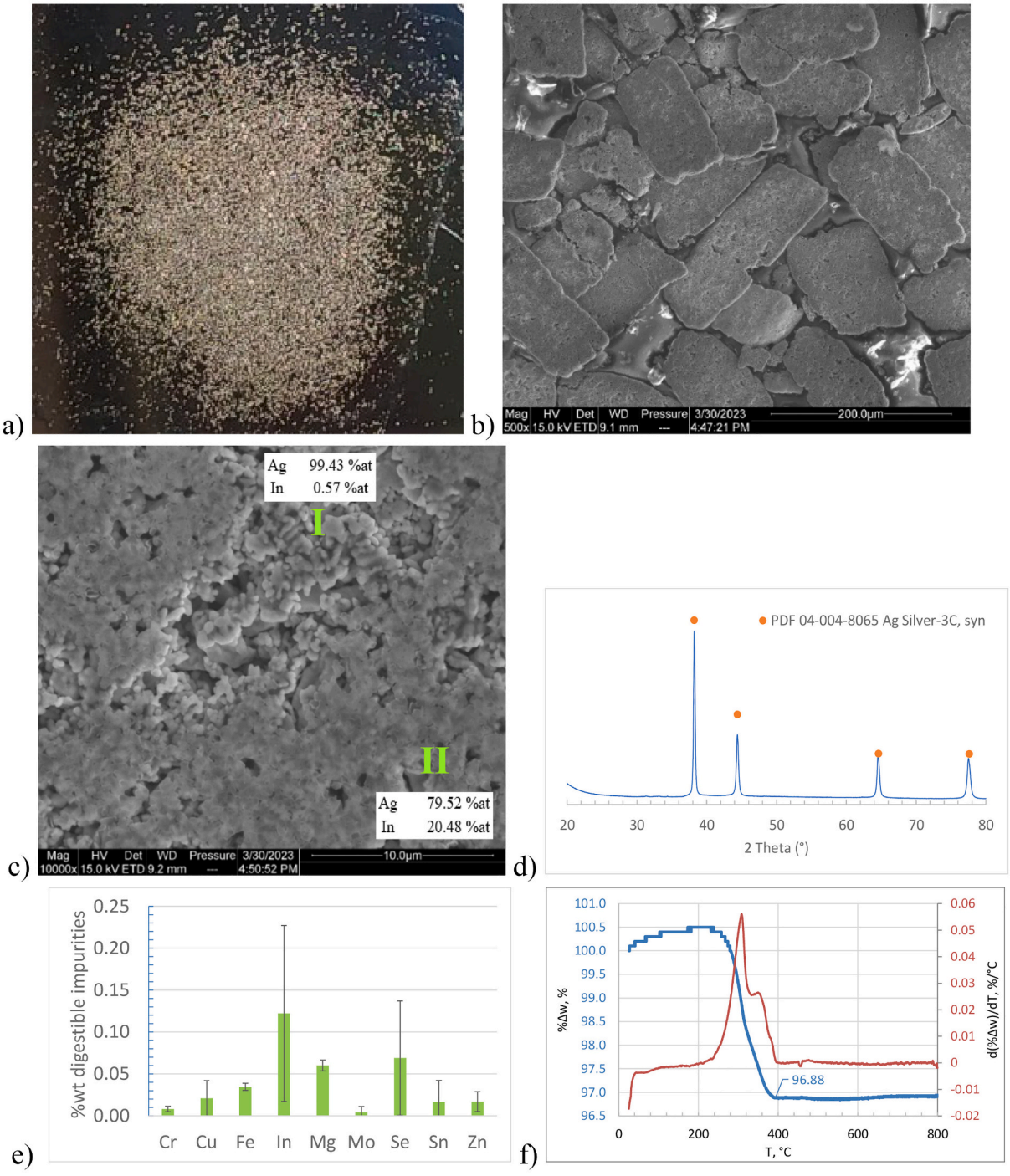

Fig. 7. Analysis of the filtered solid particles from the 2nd US-leaching step: a) recovered particles after filtration, b, c) SEM images of their morphology at higher and lower magnification, respectively, d) XRD pattern of their crystalline phases, e) elemental analysis of the digestible impurity levels expressed as wt% and f) TGA graph for quantification of organics.

Overall, the analysis showed that the recovered Ag-rich solid fraction contained 95.0 wt% Ag and 3.1 wt% organics, while the impurities coming from other elements were lower than 2 wt%. The average wt% elemental composition of the recovered Ag-rich particles is summarized in Table 1.

Regarding the % recovery of Ag, the respective digestion experiment revealed a complete recovery (the completion of the digestion is assessed in Section S9 of the Supplementary Material). More specifically, its concentration in the digestate was 72.7 ± 2.2 mg/cell. This concentration was compared to the reference total concentration of Ag in the cell, which was 64.1 ± 4.7 mg/cell [8]. The two concentrations were considered as equal, given the higher uncertainty in the determination of the latter one and manufacturing-induced differences from sample to sample, as discussed in our previous work [8]. However, due to the traces of Ag detected in the recovered ITO particles, its recovery rate was considered to be ≥99 wt%.

Finally, it is worth mentioning that, in contrast to the% Ag purity determination digestion experiments (in which the undigested particles detected in the digestion vials were the leftovers of the organics), in the % Ag recovery experiments, there was a considerable amount of

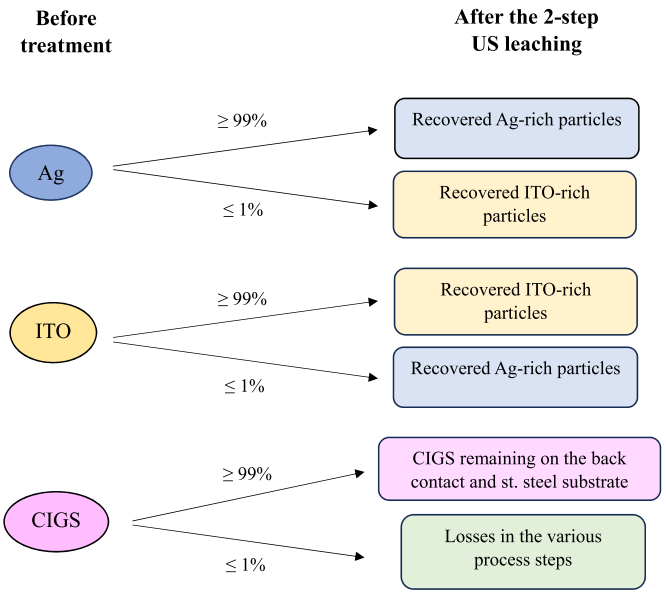

Fig. 8. Materials flow for the valuable Ag, ITO and CIGS after applying the developed 2-step US leaching process.

particles that remained undigested, even after 16 d. Their analysis with SEM-EDS revealed that those particles were again rich in Se-Fe-Cr with some S (Fig. S11 of Supplementary Material), just like in the case of the undigested fraction of the recovered ITO-rich particles. The reason why those particles were not found in the digestate of the % Ag purity determination is believed to be the use of the filter paper in combination with the big size of the Ag aggregates and the small size of these impurities. More specifically, a possible explanation is that the big size aggregates ended up on the top of the filter paper, while the small contamination particles accumulated below them and were trapped by the filter paper fibers. The dark tone of the filter papers after the recovery of the Ag particles (Fig. S9 of Supplementary Material) supports this scenario. Another fact that supports it is that the smaller size ITO-rich particles contained a much higher amount of these impurities. Therefore, filtration seems to be in this case an effective way to reduce impurity levels.

3.3. Significance and sustainability aspects of the developed recycling method

The advantages the developed method displayed are of great importance for the recycling of waste coming from CIGS solar cells for many reasons: a) the process is more environmentally friendly and less costly than the leaching methods suggested so far in the literature, due to the very low acid concentration and residence times of a few minutes required, as well as the ambient temperatures used, b) ITO can be recovered in the form of particles, meaning that the success of the method is not affected by small defects or the condition of the ITO layer, c) the complete recovery of precious Ag in high purity makes its further purification easier (since no extra separation steps are needed) and its recycling more attractive for the industry (due to the possibility of increased profits) and d) recovery of the elements which remained in the cell (In, Ga, Cu, Mo and W) is now rendered easier, due to the presence of fewer elements requiring separation and the higher possibilities for achieving higher purities for them as well. It is also worth highlighting that the developed method allowed the whole amount of the critical element Ga to remain concentrated in the CIGS layer, as it was indicated by the absence of Ga in the recovered fractions or its very low concentrations detected. The flow of the most significant materials involved in the process is visualized in Fig. 8.

So far, there is no other method developed, which can achieve such high recoveries and purities, characterized at the same time by impressively low needs in terms of chemicals and energy requirements. Therefore, this new approach opens up a new path in recycling and materials recovery using sustainable and simple methods, which can be easily adopted by the industry. Finally, recycling of whole PV modules seems to have a good chance to benefit from the developed method after proper adjustments, eg delamination of the module by the hot-knife technology [37]. Therefore, further research into the topic could be of high interest for the recycling industry.

4. Conclusions

A complete recovery of Ag and ITO particles from a flexible CIGS solar cell with a stainless steel substrate was achieved in this research work, with purities equal to 95.0 and 70.5 wt%, respectively.

The novel approach for their selective and complete recoveries in particles form was a two-step US-leaching process consisting of a 1st step at low US power and a 2nd step at high US power, with residence times of a few minutes. Only 0.1 M HNO_3 was utilized in this process, in order to remove the easily soluble Zn-rich layer placed below the Ag grid and ITO layer, and thus enabling this way their liberation from the cell. The low US power was proved suitable for selective recovery of ITO, while the high power for complete recovery of the Ag. The characterization of the recovered ITO-rich particles showed that they maintained their crystalline ITO phase, while the majority of impurities present was a non-digestible material, rich in Se-Fe-Cr and some S, probably coming from manufacturing residues on the stainless steel substrate. Ag also maintained its crystalline metal structure, but the main impurity detected there was the organic residues from the Ag paste, at a level of 3.1 wt%. The Ag was proved to have been recovered in the form of aggregated particles, still attached on grid line fragments, with some pieces of ITO remaining attached on the latter. However, the In content of the Ag-rich particles was only about 0.1 wt%.

It is believed that the high purity of the recovered Ag and its low content in inorganic impurities can partly be attributed to the fact that Ag was recovered as large fragments of the conductive grid. The size of the fragments facilitated their separation from the filter paper by washing and left the small impurity particles trapped in the filter, increasing the purity of Ag.

In total, with regard to the simultaneous high recovery and high purity of the valuable materials achieved with the method, in combination with its simplicity, low chemicals content, short residence times and low effect of the process on other valuable materials which can be recovered at later stages, the developed method is an attractive alternative for recycling of Ag and ITO with the purpose of reusing them into new solar cells. For this purpose, however, the method must first be optimized for a larger scale use.

CRediT authorship contribution statement

Ioanna Teknetzi: Writing – original draft, Visualization, Validation, Methodology, Investigation, Formal analysis. **Natalie Click:** Writing – review & editing. **Stellan Holgersson:** Writing – review & editing, Supervision. **Burçak Ebin:** Writing – review & editing, Supervision, Resources, Project administration, Methodology, Funding acquisition, Conceptualization.

Declaration of competing interest

None.

Data availability

Data will be made available on request.

Acknowledgements

This work was funded by the Swedish Energy Agency [P2019-90193] (without any involvement from their side in the conduction of research and preparation of the article). The authors would also like to thank Midsummer AB for kindly providing the solar cell samples. Finally, the authors would like to acknowledge the Chalmers Materials Analysis Laboratory, CMAL, for providing their facilities and assistance with the SEM-EDS and XRD analysis.

Appendix A. Supplementary Data

Supplementary data to this article can be found online at https://doi.org/10.1016/j.susmat.2024.e00844.

References

[1] The Silver Institute, World Silver survey 2022, Available at: https://www.silverinstitute.org/wp-content/uploads/2022/04/World-Silver-Survey-2022.pdf, 2022 (Accessed 2nd July 2023).
[2] U.S. Geological Survey, Mineral commodity summaries 2022: U.S, Geological Survey (2022) 202, https://doi.org/10.3133/mcs2022.
[3] A. Elshkaki, T.E. Graedel, Solar cell metals and their hosts: a tale of oversupply and undersupply, Appl. Energy 158 (2015) 167–177, https://doi.org/10.1016/j.apenergy.2015.08.066.
[4] N. Moudir, Y. Boukennous, N. Moulaï-Mostefa, I. Bozetine, M. Maoudj, N. Kamel, Z. Kamel, D. Moudir, Preparation of silver powder used for solar cell paste by reduction process, N. Moudir, Energy Procedia 36 (2013) 1184–1191, https://doi.org/10.1016/j.egypro.2013.07.134.
[5] Fraunhofer Institute for Solar Energy Systems, Photovoltaics Report, available at, https://www.ise.fraunhofer.de/content/dam/ise/de/documents/publications/studies/Photovoltaics-Report.pdf, 2022 (Accessed 22nd May 2023).
[6] X. Wang, X. Tian, X. Chen, L. Ren, C. Geng, A review of end-of-life crystalline silicon solar photovoltaic panel recycling technology, Sol. Energy Mater. Sol. Cells 248 (2022) 111976, https://doi.org/10.1016/j.solmat.2022.111976.
[7] J.-P. Wang, D.-H. Lee, M.-S. Go, E.-K. So, A study on the wet process conditions that affect the selective recovery of Si from photovoltaic cells by using the cavitation effect, Metals 12 (2) (2022) 222, https://doi.org/10.3390/met1202022.
[8] I. Teknetzi, S. Holgersson, B. Ebin, Valuable metal recycling from thin film CIGS solar cells by leaching under mild conditions, Sol. Energy Mater. Sol. Cells 252 (2023) 112178, https://doi.org/10.1016/j.solmat.2022.112178.
[9] S. Virolainen, D. Ibana, E. Paatero, Recovery of indium from indium tin oxide by solvent extraction, Hydrometall. 107 (1–2) (2011) 56–61, https://doi.org/10.1016/j.hydromet.2011.01.005.
[10] International Energy Agency, Final List of Critical Minerals 2022, Available at: https://www.iea.org/policies/15271-final-list-of-critical-minerals-2022, 2023 (Accessed 30 June 2023).
[11] J. Schuster, B. Ebin, Investigation of indium and other valuable metals leaching from unground waste LCD screens by organic and inorganic acid leaching, Sep. Purif. Technol. 279 (2021) 119659, https://doi.org/10.1016/j.seppur.2021.119659.
[12] U.S. Geological Survey, Mineral Commodity Summaries 2023: U.S. Geological Survey, 2023, p. 210, https://doi.org/10.3133/mcs2023.
[13] J. Yang, T. Retegan, C. Ekberg, Indium recovery from discarded LCD panel glass by solvent extraction, Hydrometall 137 (2013) 68–77, https://doi.org/10.1016/j.hydromet.2010.09.006.
[14] Y. Li, Z. Liu, Q. Li, Z. Liu, L. Zeng, Recovery of indium from used indium–tin oxide (ITO) targets, Hydrometall 105 (3–4) (2011) 207–212, https://doi.org/10.1016/j.hydromet.2010.09.006.
[15] K.N. Han, S. Kondoju, K. Park, Ho-min Kang, Recovery of indium from indium/tin oxides scrap by chemical precipitation, Geosystem Eng. 5 (4) (2002), https://doi.org/10.1080/12269328.2002.10541193.
[16] K. Zhang, B. Li, Y. Wu, W. Wang, R. Li, Y.-N. Zhang, T. Zuo, Recycling of indium from waste LCD: a promising non-crushing leaching with the aid of ultrasonic wave, Waste Manag. 64 (2017) 236–243, https://doi.org/10.1016/j.wasman.2017.03.031.
[17] M. Souada, C. Louage, J.-Y. Doisy, L. Meunier, A. Benderrag, B. Ouddane, S. Bellayer, N. Nuns, M. Traisnel, U. Maschke, Extraction of indium-tin oxide from end-of-life LCD panels using ultrasound assisted acid leaching, Ultrason. Sonochem. 40 (A) (2018) 929–936, https://doi.org/10.1016/j.ultsonch.2017.08.043.
[18] B. Augustine, K. Remes, G.S. Lorite, J. Varghese, T. Fabritius, Recycling perovskite solar cells through inexpensive quality recovery and reuse of patterned indium tin oxide and substrates from expired devices by single solvent treatment, Sol. Energy Mater. Sol. Cells 194 (2019) 74–82, https://doi.org/10.1016/j.solmat.2019.01.041.
[19] B. Chen, C. Fei, S. Chen, H. Gu, X. Xiao, J. Huang, Recycling lead and transparent conductors from perovskite solar modules, Nat. Commun. 12 (2021), https://doi.org/10.1038/s41467-021-26121-1. Article number: 5859.
[20] R. Hu, X. Su, H. Liu, Y. Liu, M.-M. Huo, W. Zhang, Recycled indium tin oxide transparent conductive electrode for polymer solar cells, J. Mater. Sci. 55 (2020) 11403–11410, https://doi.org/10.1007/s10853-020-04825-x.
[21] M. Elshobaki, J. Anderegg, S. Chaudhary, Efficient polymer solar cells fabricated on poly(3,4-ethylenedioxythiophene):poly-(styrenesulfonate)-etched old indium tin oxide substrates, ACS Appl. Mater. Interfaces 6 (2014) 12196–12202, https://doi.org/10.1021/am5037884.
[22] M.T. Dang, P.-L.M. Brunner, J.D. Wuest, A green approach to organic thin-film electronic devices: recycling electrodes composed of indium tin oxide (ITO), ACS Sustain. Chem. Eng. 2 (2014) 2715–2721, https://doi.org/10.1021/sc500456p.
[23] M.T. Dang, J. Lefebvre, J.D. Wuest, Recycling indium tin oxide (ITO) electrodes used in thin-film devices with adjacent hole-transport layers of metal oxides, ACS Sustain. Chem. Eng. 3 (12) (2015) 3373–3381, https://doi.org/10.1021/acssuschemeng.5b01080.
[24] International Energy Agency (IEA), Solar PV, available at, https://www.iea.org/energy-system/renewables/solar-pv, 2023 (Accessed 8th January 2024).
[25] F.-W. Liu, T.-M. Cheng, Y.-J. Chen, K.-C. Yueh, S.-Y. Tang, K. Wang, C.-L. Wu, H.-S. Tsai, Y.-J. Yu, C.-H. Lai, W.-S. Chen, Y.-L. Chueh, High-yield recycling and recovery of copper, indium, and gallium from waste copper indium gallium selenide thin-film solar panels, Sol. Energy Mater. Sol. Cells 241 (2022) 111691, https://doi.org/10.1016/j.solmat.2022.111691.
[26] A. Amato, F. Beolchini, End-of-life CIGS photovoltaic panel: a source of secondary indium and gallium, Prog. Photovolt. 27 (2019) 229–236, https://doi.org/10.1002/pip.3082.
[27] Y. Lv, P. Xing, B. Ma, B. Liu, C. Wang, Y. Zhang, W. Zhang, Separation and recovery of valuable elements from spent CIGS materials, ACS Sustain. Chem. Eng. 7 (24) (2019) 19816–19823, https://doi.org/10.1021/acssuschemeng.9b05121.
[28] H.-I. Hsiang, C.-Y. Chiang, W.-H. Hsu, W.-S. Chen, J.-E. Chang, Leaching and resynthesis of CIGS nanocrystallites from spent CIGS targets, Adv. Powder Technol. 27 (3) (2016) 914–920, https://doi.org/10.1016/j.apt.2016.02.012.
[29] S. Gu, B. Fu, G. Dodbiba, T. Fujita, B. Fang, Promising approach for recycling of spent CIGS targets by combining electrochemical techniques with dehydration and distillation, ACS Sustain. Chem. Eng. 6 (5) (2018) 6950–6956. https://pubs.acs.org/doi/10.1021/acssuschemeng.8b00787.
[30] I. Teknetzi, Recycling of CIGS Solar Cells: Environmentally Friendly Approaches for Silver and Indium Recovery, Chalmers University of Technology, Sweden, 2023. Licentiate thesis, https://research.chalmers.se/publication/537899/file/537899_Fulltext.pdf.
[31] X. Li, Z. Deng, C. Li, C. Wei, M. Li, G. Fan, H. Rong, Direct solvent extraction of indium from a zinc residue reductive leach solution by D2EHPA, Hydrometall 156 (2015) 1–5, https://doi.org/10.1016/j.hydromet.2015.05.003.
[32] B. Huang, X. Li, Y. Pei, S. Li, X. Cao, R.C. Mass, G. Cao, Novel carbon-encapsulated porous SnO2 anode for lithium-ion batteries with much improved cyclic stability, Small 12 (14) (2016) 1945–1955, https://doi.org/10.1002/smll.201503419.
[33] P.C. Huang, C.C. Sung, J.H. Chen, R.C. Hsiao, C.Y. Hsu, Effect of selenization and sulfurization on the structure and performance of CIGS solar cell, J. Mater. Sci. Mater. Electron. 29 (2018) 1444–1450, https://doi.org/10.1007/s10854-017-8052-6.
[34] V.A. Lavrenko, A.I. Malyshevskaya, L.I. Kuznetsova, V.F. Litvinenko, V.N. Pavlikov, Features of high-temperature oxidation in air of silver and alloy ag – cu, and adsorption of oxygen on silver, Powder Metall. Met. Ceram. 45 (2006) 476–480, https://doi.org/10.1007/s11106-006-0108-8.
[35] Q. Sun, Y. Qi, M. Li, H. Xu, Y. Li, Synthesis of PVZ glass and its improvement on mechanical and electrical properties of low temperature sintered silver paste, J. Mater. Sci. Mater. Electron. 31 (2020) 8086–8098, https://doi.org/10.1007/s10854-020-03349-z.
[36] G. Bárcenas-Moreno, E. Jiménez-Compán, L.M. San Emeterio, N.T. Jiménez-Morillo, J.A. González-Pérez, Soil pH and soluble organic matter shifts exerted by heating affect microbial response, Int. J. Environ. Res. Public Health 19 (23) (2022) 15751, https://doi.org/10.3390/ijerph192315751.
[37] B. Sauer, Advancing circular economy in photovoltaics: The Hot Knife PV module recycling method, PV magazine, available at, https://www.pv-magazine.com/2023/08/17/advancing-circular-economy-in-photovoltaics-the-hot-knife-pv-module-recycling-method/, 2023 (Accessed 9th January 2024).